Available online at www.sciencedirect.com
ScienceDirect
Journal of Organometallic Chemistry 692 (2007) 166–174
Journal of Organometallic Chemistry
www.elsevier.com/locate/jorganchem

# Synthesis and structures of cobalt(II) complexes of *meso*-tetraphenyloctaphyrin(1.0.1.0.1.0.1.0)s

Jun-ichiro Setsune *, Megumi Mori, Toshifumi Okawa, Satoshi Maeda, Juha M. Lintuluoto

*Department of Chemistry, Faculty of Science, and Graduate School of Science and Technology, Kobe University, Nada-ku, Kobe 657-8501, Japan*

Received 1 March 2006; received in revised form 5 April 2006; accepted 7 April 2006
Available online 30 August 2006

**Abstract**

Some *meso*-tetraphenyloctaphyrin(1.0.1.0.1.0.1.0)s and their Co(II) complexes were prepared and characterized on the basis of the $^1$H NMR spectra and X-ray crystallography. These octaphyrins have a figure eight structure. The methyl and methylene protons directly bound to the bipyrrole β-position at the crossing point of the figure eight loop were very close to Co(II) and showed their $^1$H NMR resonances in the range of 30–300 ppm. The insertion of Co(II) into the octaphyrin with mixed 2,2′-bipyrrole units of different substitution pattern induced transposition of the sterically more congested 2,2′-bipyrrole unit from the crossing point of the figure eight loop to the periphery.


*Keywords:* Cobalt complex; Porphyrinoid; Octaphyrin

## 1. Introduction

A number of reports on the expanded porphyrins have been appearing and their properties are discussed from the viewpoints of photochemistry, supramolecular chemistry, and coordination chemistry [1,2]. We have recently developed efficient synthetic methods for *meso*-tetraaryloctaphyrin(1.0.1.0.1.0.1.0)s [3]. Octaphyrin(1.0.1.0.1.0.1.0) is composed of four parts of 2,2′-bipyrrole linked by four *meso*-carbons. Although bulky substituents at the 3,3′-position of 2,2′-bipyrrole are favored for the efficient cyclization reaction to take place [3a], they are expected to make steric hindrance in the metal insertion and the axial coordination of the metal complexes of octaphyrin. Metal complexes of octaphyrins have been drawing great attention due to their unique stereochemical and electrochemical features [4–9]. In order to prepare octaphyrins suitable for studying coordination chemistry, 2,2′-bipyrrole without substituents at the 3,3′-position is preferable. In view of the efficiency in the cyclization reaction we planned to prepare octaphyrin(1.0.1.0.1.0.1.0) containing mixed bipyrrole units. Selective syntheses of porphyrinoids with an alternate ABAB arrangement of two different building blocks are problematic especially in the case of *meso*-aryl type porphyrinoids, because the acid catalyzed reaction conditions generally used for the cyclization cause scrambling of the two building blocks [10]. We describe in this paper the synthesis of *meso*-tetraphenyloctaphyrin(1.0.1.0.1.0.1.0) without substituents at the 3,3′-position of the 2,2′-bipyrrole units by using bis(azafulvene) under neutral conditions [3a,3c,11]. It is of interest to see how the variation of the alkyl substituents at the pyrrole β-positions influences the structure not only of the octaphyrin(1.0.1.0.1.0.1.0) free base but also of the corresponding metal complexes. Whereas the electrochemical properties of Co(II) octaphyrins have been studied by Vogel and coworkers [9], their structures and spectroscopic properties have not been well understood. Thus, we have decided to investigate the Co(II) complexes of *meso*-tetraphenyloctaphyrin(1.0.1.0.1.0.1.0)s in this work.

* Corresponding author. Fax: +81 78 803 5770.
*E-mail address:* setsunej@kobe-u.ac.jp (J.-i. Setsune).

0022-328X/$ - see front matter © 2006 Elsevier B.V. All rights reserved.
doi:10.1016/j.jorganchem.2006.04.045

## 2. Results and discussion

### 2.1. Synthesis and structures of octaphyrin(1.0.1.0.1.0.1.0)s

Vogel and coworkers reported that octaphyrin(1.0.1.0.1.0.1.0) was prepared by MacDonald [2+2]-type condensation reaction of bipyrrole dialdehyde with bipyrrole dicarboxylic acid or α-free bipyrrole under acidic conditions [2c,4]. We have previously reported that the addition reaction of α-free bipyrrole and bis(azafulvene) under neutral conditions gives octaphyrin as a principal product along with larger cyclopolypyrroles after oxidative work-up [3a,11]. This is a versatile synthetic method for *meso*-tetraaryloctaphyrin(1.0.1.0.1.0.1.0)s. 4,4′-Dipropyl-2,2′-bipyrrole **1a** was converted to the dialdehyde by Vilsmeier reaction and then to 5,5′-bis(phenylhydroxymethyl)-2,2′-bipyrroles **2a** by using phenyllithium. The bipyrrole dicarbinol **2a** was then reacted with di-*t*-butyl dicarbonate ($Boc_2O$) in the presence of *N*,*N*-dimethylaminopyridine (DMAP) to give 82% yield of bis(azafulvene) **3a**. Bis(azafulvene) **3b** was prepared from 4,4′-diethyl-3,3′-dimethyl-2,2′-bipyrrole **1b** in 60% total yield by way of the corresponding bipyrrole dicarbinol **2b**. The reaction of **1b** and **3b** under neutral conditions afforded 2,7,11,16,20,25,29,34-octaethyl-3,6,12,15,21,24,30,33-octamethyl-9,18,27, 36-*meso*-tetraphenyloctaphyrin(1.0.1.0.1.0.1.0) **4b** in 39% yield after oxidation with 2,3-dichloro-5,6-dicyanobenzoquinone (DDQ) (see Scheme 1). This reaction did not afford hexapyrrolic macrocycle called rosarin which was synthesized by the acid catalyzed condensation of **1b** with benzaldehyde in 70% yield [2a]. When bis(azafulvene) **3a** was allowed to react with 3,3′-di-*iso*-butyl-4,4′-dimethyl-2,2′-bipyrrole [11] **1c** at room temperature for 24 h, 2,7,20,25-tetrapropyl-11,16,29,34-tetramethyl-12,15,30,33-tetra-*iso*-butyl-9, 18,27,36-*meso*-tetraphenyloctaphyrin(1.0.1.0.1.0.1.0) **4a** was obtained similarly in 28% yield (see Scheme 1). Since bipyrrole is an electron donor and bis(azafulvene) is an electron acceptor in this addition reaction, the combination of **1c** and **3a** should be better than the reverse combination of 2,2′-bipyrrole **1a** and bis(azafulvene) derived from **1c**. Tetraalkylated bipyrrole **1c** is more reactive as a donor than the dialkylated bipyrrole **1a**.

X-ray crystallography of **4a** showed a figure eight type structure previously reported by Vogel and coworkers for 2,3,6,7,11,12,15,16,20,21,24,25,29,30,33,34-hexadecaethyloctaphyrin(1.0.1.0.1.0.1.0) **4** where two bipyrrole units in a *trans* $N–C_\alpha–C_\alpha–N$ conformation are at the crossing point of the figure eight loop and two bipyrrole units in a *cis* $N–C_\alpha–C_\alpha–N$ conformation are at the periphery [2c]. The *iso*-butyl-substituted bipyrrole is positioned at the crossing point of the figure eight loop of **4a**, probably because the steric constraint between the bulky 3,3′-di-*iso*-butyl groups renders the bipyrrole conformation *trans*. Table 1 shows that the $N–C_\alpha–C_\alpha–N$ torsion angles in the *cis*-4,4′-dipropyl-2,2′-bipyrrole units of **4a** (12.0° and 1.9°) are smaller than those in the *cis*-3,3′,4,4′-tetraethyl-2,2′-bipyrrole units of **4** (34.8° and 34.0°) and the $N–C_\alpha–C_\alpha–N$ torsion angles in the *trans*-3,3′-di-*iso*-butyl-4,4′-dimethyl-2,2′-bipyrrole units of **4a** (162.8° and 164.1°) are larger than those in the *trans*-3,3′,4,4′-tetraethyl-2,2′-bipyrrole units of **4**

Table 1
Torsion angles (°) of the bipyrrole units ($N–C_\alpha–C_\alpha–N$) and of the dipyrrylmethene units ($C_\alpha–C_{meso}–C_\alpha–N$ and $N–C_\alpha–C_{meso}–C_\alpha$) for **4a** and **4**[a]

| | **4a** | | | **4** | | | | |
|---|---|---|---|---|---|---|---|---|
| $N–C_\alpha–C_\alpha–N$ | 12.0 | 162.8 | 1.9 | 164.1 | 34.8 | 151.8 | 34.0 | 150.8 |
| $C_\alpha–C_{meso}–C_\alpha–N$ | 15.3 | 12.5 | 14.3 | 13.0 | 7.5 | 3.9 | 4.0 | 1.8 |
| $N–C_\alpha–C_{meso}–C_\alpha$ | 26.2 | 15.0 | 12.5 | 13.7 | 1.8 | 6.4 | 5.8 | 6.8 |

[a] The data of **4** were taken from Ref. [2c].

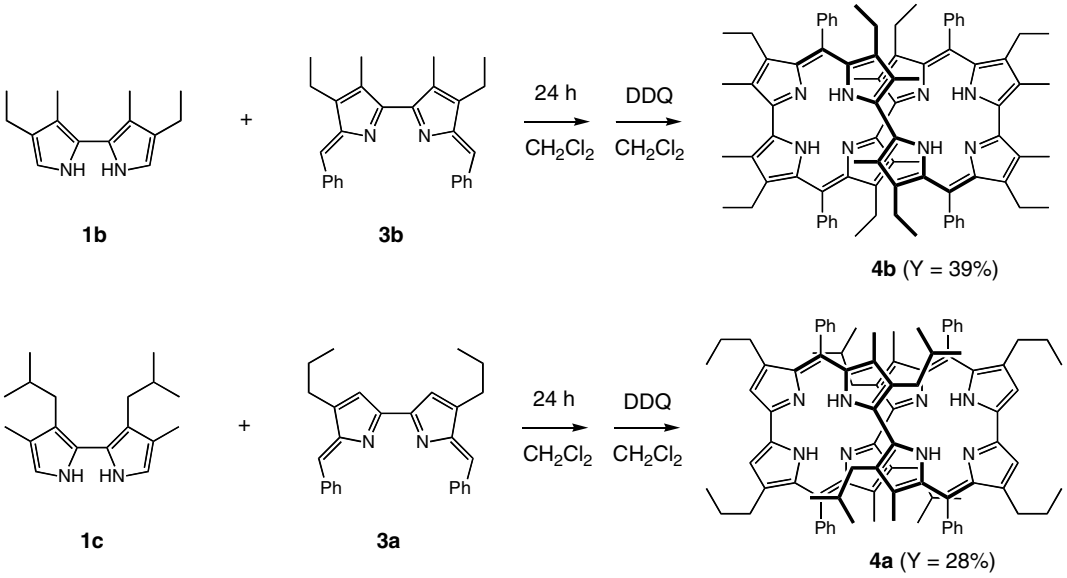


Scheme 1. Synthesis of octaphyrin(1.0.1.0.1.0.1.0) **4a** and **4b**.

(151.8° and 150.8°). This leads to the rectangle shaped cavity for **4a** in contrast to the rhombus shape for **4** as shown in Fig. 1. Table 1 also summarizes the torsion angles $C_{\alpha}$–$C_{meso}$–$C_{\alpha}$–N and N–$C_{\alpha}$–$C_{meso}$–$C_{\alpha}$ which are diagnostic of the planarity of the dipyrrylmethene units. While the planarity of the dipyrrylmethene units is kept to the sacrifice of the planarity of the bipyrrole units in the case of **4**, the planarity of the bipyrrole units are kept to the sacrifice of the planarity of the dipyrrylmethene units in the case of **4a**. The *iso*-butyl groups are directed inwards the molecular cavity and the methine proton of the *iso*-butyl group is close to the pyrrole nitrogen of the propyl-substituted bipyrrole with an estimated distance of 2.77 Å.

The 2D ROESY NMR spectrum of **4a** at 20 °C in toluene-$d_8$ showed an intense correlation between the NH signal at 14.92 ppm and one of the two methyl signals of the *iso*-butyl group at 1.01 ppm (see Supplementary material). This NOE effect would be impossible to observe if the *iso*-butyl groups were at the periphery of the figure eight loop in solution. Variable temperature $^1$H NMR spectra of **4a** between +80 °C and −60 °C in toluene-$d_8$ showed only one set of signals, which means that a single conformational isomer is present or the interconversion between some conformational isomers are very fast on the NMR time scale even at −60 °C. While the chemical shifts of the propyl protons and the β-pyrrole proton are only slightly affected by less than 0.05 ppm in the whole temperature range, signals due to the *iso*-butyl group underwent remarkable chemical shift changes with decreasing temperature from +80 °C to −60 °C as shown in Fig. 2. Two methyl doublets, a methine multiplet ($H_c$), and one of the diastereotopic methylene multiplets ($H_a$) were shifted to the higher frequency region by 0.58, 1.05, 1.54, and 0.66 ppm, respectively, while the other methylene proton signal ($H_b$) moved to the lower frequency region by 0.73 ppm. On the other hand, the methyl singlet due to the β-pyrrole position was not sensitive to temperature with the total chemical shift change less than 0.1 ppm. The remarkable temperature dependency specifically found for the *iso*-butyl group strongly indicates that the figure eight conformation with the 3,3′-di-*iso*-butyl-4,4′-dimethyl-2,2′-bipyrrole units at the crossing point of the figure eight loop is predominant in solution and that the *iso*-butyl group comes closer to the propyl-substituted bipyrrole as temperature goes down probably by rotating around the $C_{(butyl)}$–$C_{(pyrrole\text{-}\beta)}$ bond.

### 2.2. Co(II) complexes of octaphyrin(1.0.1.0.1.0.1.0)s

Mononuclear Co(II) complexes of *meso*-tetraphenyloctaphyrin(1.0.1.0.1.0.1.0)s were readily prepared when a methanol solution of Co(II) acetate was reacted with a

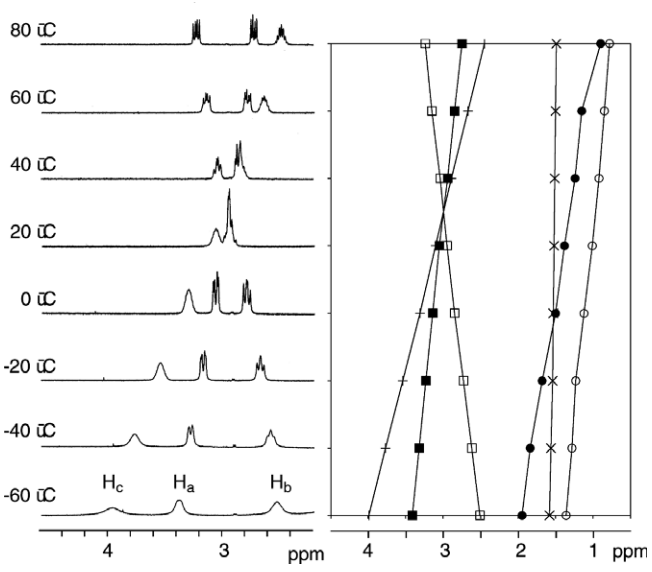


Fig. 2. Variable temperature $^1$H NMR spectra in the region of the *iso*-butyl-$CH_2$ ($H_a$ and $H_b$) and the *iso*-butyl-CH ($H_c$) of **4a** in toluene-$d_8$ (left) and a plot of the proton chemical shifts due to the 4-*iso*-butyl-3-methylpyrrole moiety with temperature (right). open and filled circles: *iso*-butyl-Me, cross: pyrrole-β-Me, open and filled squares: *iso*-butyl-$CH_2$, plus: *iso*-butyl-CH.

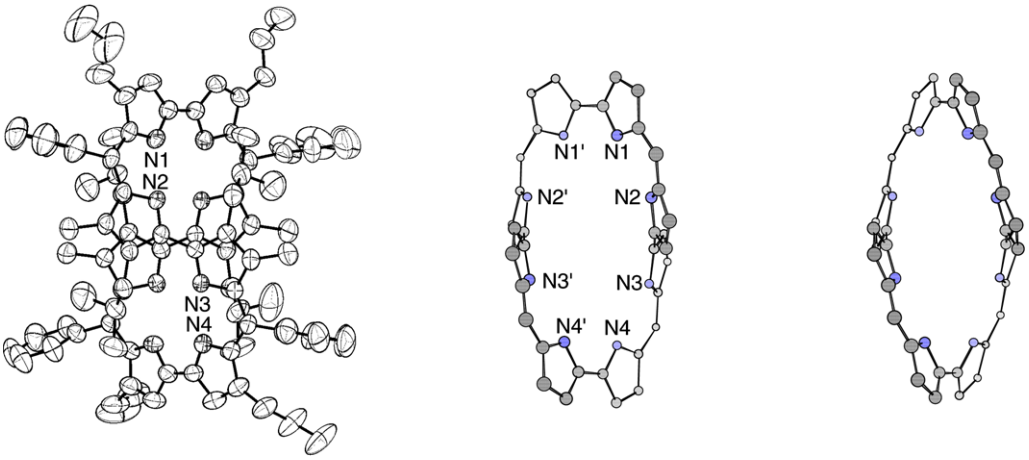


Fig. 1. A 50% level Ortep drawing of **4a** (left); a side view of **4a** without peripheral substituents (middle) in comparison with that of **4** (right).

$CHCl_3$ solution of octaphyrin. The monocobalt(II) complexes **4a-Co**, **4b-Co**, **4c-Co**, and **4d-Co** were obtained in 57%, 66%, 59%, and 45% yield from **4a**, **4b**, 2,7,11,16,-20,25,29,34-octamethyl-3,6,12,15,21,24,30,33-octa-*iso*-butyl-9,18,27,36-*meso*-tetraphenyloctaphyrin(1.0.1.0.1.0.1.0) **4c**, and 2,3,6,7,11,12,15,16,20,21,24,25,29,30,33,34-hexadecaethyl-9,18,27,36-*meso*-tetraphenyloctaphyrin(1.0.1.0.1.0.1.0) **4d** [3b], respectively (see Scheme 2). The insertion of the second Co(II) required temperature more than 120 °C in the reaction of **4b** and **4d** with Co(II) acetylacetonate in phenol and the dinuclear complexes, **4b-Co$_2$** and **4d-Co$_2$**, were obtained in 28% and 33% yield, respectively.

The absorption band of the free base **4b** at 578 nm underwent red shift to 588 nm for the monocobalt complex **4b-Co** and to 597 nm for the dicobalt complex **4b-Co$_2$** as depicted in Fig. 3. The $^1$H NMR spectrum of **4b-Co$_2$** showed 13 signals in the 75 ppm total range (see Fig. 4) and they were unambiguously assigned as summarized in Table 2 with the aid of $^1$H–$^1$H COSY NMR experiment (see Fig. 5). The signal at −51.0 ppm of **4b-Co$_2$** is associated with the pyrrole β-methyl protons in the *trans*-bipyrrole unit at the crossing point of the figure eight loop, because these methyl protons are subject to very large dipolar shift by Co(II) in the close proximity. The signal at 23.8 ppm is associated with the pyrrole β-methyl protons in the *cis*-bipyrrole unit at the periphery and the contact shift caused by Co(II) should be mainly responsible for this

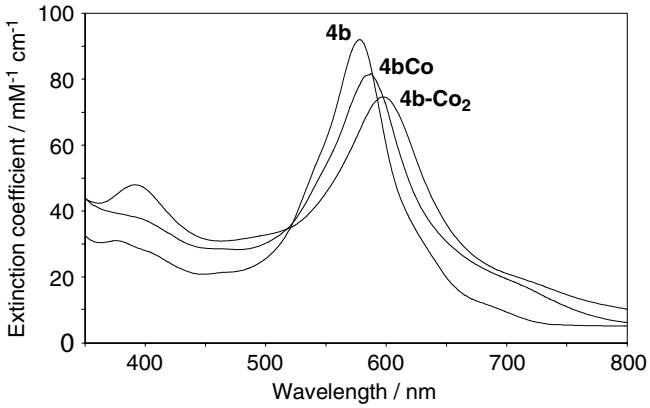


Fig. 3. UV–Vis spectra of **4b**, **4b-Co**, and **4b-Co$_2$** in $CH_2Cl_2$.

high frequency shift. The $^1$H NMR signals of **4b-Co** were assigned on the basis of the $^1$H–$^1$H COSY experiment and the chemical shifts of the corresponding protons determined for **4b-Co$_2$**. The signal at −64.4 ppm due to the pyrrole β-methyl protons close to Co(II) is by 13.4 ppm lower frequency than the corresponding signal of **4b-Co$_2$**. Therefore, the effect of Co(II) bound at the pyrrole nitrogen on the β-methyl protons of the same pyrrole can be estimated as 13.4 ppm to the high frequency region. A signal at 43.9 ppm of **4b-Co** disappeared by adding a drop of $D_2O$ and thus was associated with the NH proton of the mon-

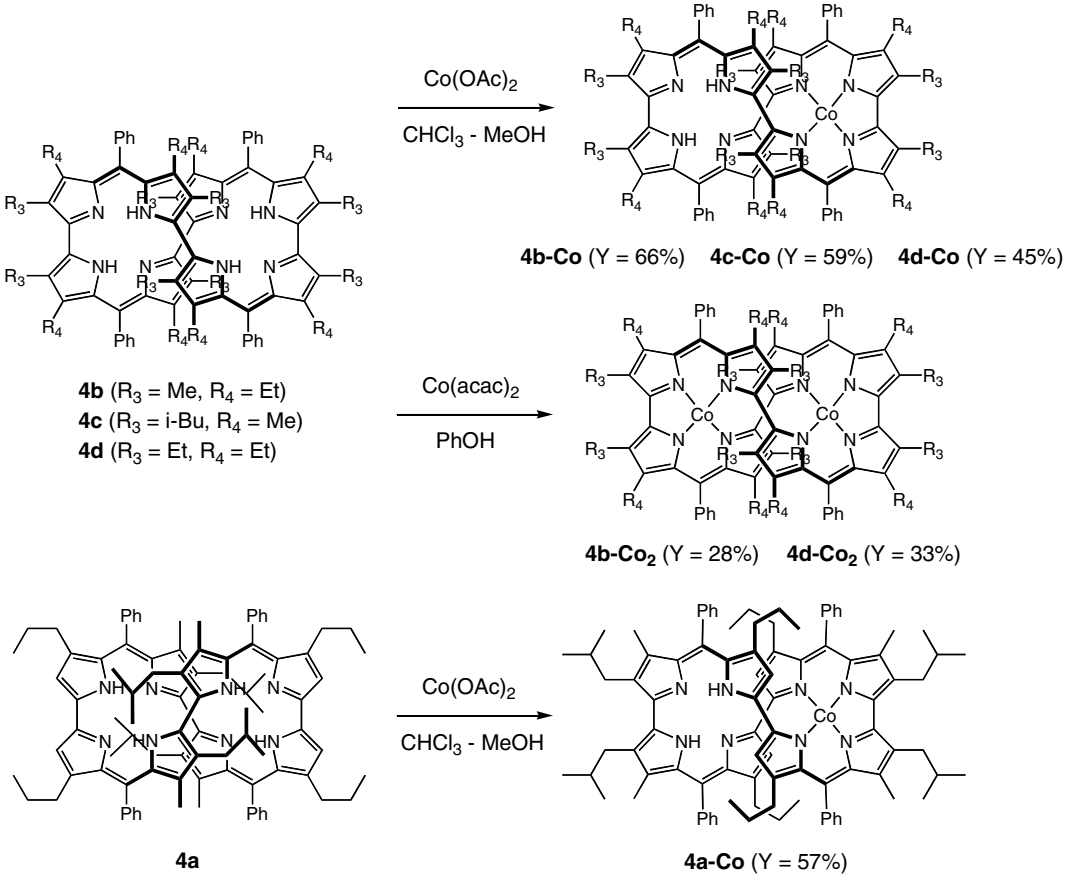


Scheme 2. Synthesis of Co(II) complexes of octaphyrin(1.0.1.0.1.0.1.0)s **4a**, **4b**, **4c**, and **4d**.

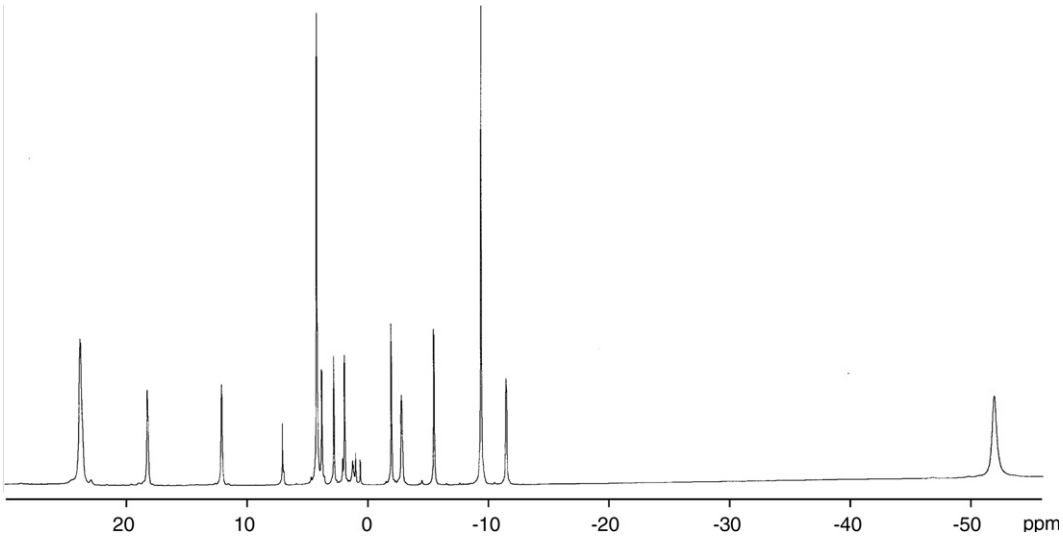


Fig. 4. $^1$H NMR spectrum of **4b-Co$_2$** in $CDCl_3$ at 20 °C.

Table 2
$^1$H NMR chemical shifts of **4b-Co**, **4b-Co$_2$**, and **4d-Co$_2$** in $CDCl_3$ at 20 °C

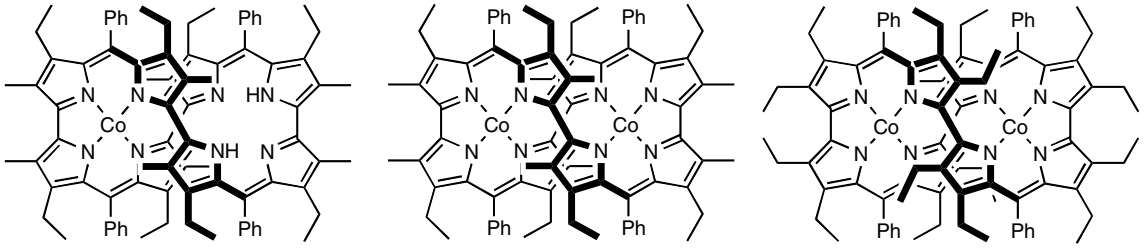


| | **4b-Co** | | | | **4b-Co$_2$** | | **4d-Co$_2$** | | | |
|---|---|---|---|---|---|---|---|---|---|---|
| $CH_3$ | 25.6 | 18.8 | 7.4 | −64.4 | 23.8 | −51.0 | | | | |
| $CH_2CH_3$ | 16.6 | 4.6 | 3.5 | −2.4 | 18.3 | −2.6 | 29.1 | 18.8 | −0.2 | −30.5 |
| | 11.0 | 4.0 | −3.6 | −7.1 | 12.2 | −11.1 | 24.9 | 15.5 | −9.5 | −176 |
| $CH_2CH_3$ | 1.8 | 2.8 | −0.5 | −5.6 | 4.4 | −9.1 | 18.8 | 3.5 | −8.6 | −15.4 |
| $C_6H_5$-*o* | 10.5 | 9.1 | −3.3 | −7.1 | −1.7 | −5.2 | −0.9 | −4.7 | | |
| $C_6H_5$-*m* | 7.3 | 7.3 | 3.0 | 2.4 | 3.0 | 2.1 | 2.9 | 1.6 | | |
| $C_6H_5$-*p* | 7.2 | | 4.5 | | 4.0 | | 4.3 | | | |
| NH | 43.9 | | | | | | | | | |

ocobalt complex. The $^1$H chemical shifts of **4d-Co$_2$** are similar to those of **4b-Co$_2$** except for the pyrrole β-ethyl groups that replaced the pyrrole β-methyl groups of **4b-Co$_2$**. The signals at −176, −30.5, and −15.4 ppm with the 1:1:3 relative intensity of **4d-Co$_2$** are associated with the pyrrole β-ethyl protons close to Co(II), while the corresponding pyrrole β-ethyl protons appeared at −205, −35.5, and −19.3 ppm in the case of the monocobalt complex **4d-Co**. These very low frequency chemical shifts at around −200 ppm indicate that one of the diastereotopic methylene protons of the pyrrole β-ethyl group is very close to Co(II). The extremely low frequency signals at −294 and −54.5 ppm observed for **4c-Co** are also associated with the diastereotopic methylene protons of the *iso*-butyl group close to Co(II). Since the ratio of the isotropic shifts for the diastereotopic methylene protons is 5.5 for **4d-Co** and **4d-Co$_2$** and 5.3 for **4c-Co**, the stereochemical relationship of these two protons with respect to Co(II) is similar for these Co(II) complexes. This is because the dipolar shift depends on the geometric factor $(3\cos^2\theta - 1)/r^3$ where $r$ is the distance between Co(II) and H and $\theta$ is the angle of the Co(II)-to-H direction with respect to the principal axis of the spin tensor [12]. The intense signals at −9.0, and −13.8 ppm of **4c-Co** are associated with the methyl proton of the *iso*-butyl group close to Co(II). These low frequency resonances are characteristic of the *iso*-butyl group at the crossing point of the figure eight loop in the Co(II) octaphyrins. However, **4a-Co** did not show these low frequency resonances as depicted in Fig. 6. Therefore, the 4,4′-dipropyl-2,2′-bipyrrole unit is at the crossing point of the figure eight loop and 3,3′-di-*iso*-butyl-4,4′-dimethyl-2,2′-bipyrrole unit is at the periphery in the case of **4a-Co**. It is of

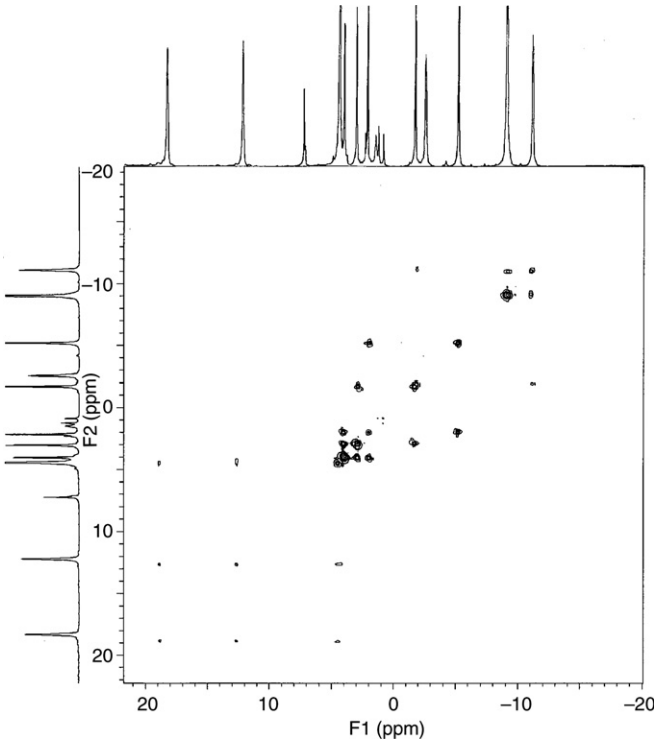


Fig. 5. $^{1}H$–$^{1}H$ COSY NMR spectrum of **4b-Co$_2$** in the chemical shift range of +20 to −20 ppm in $CDCl_3$ at 20 °C.

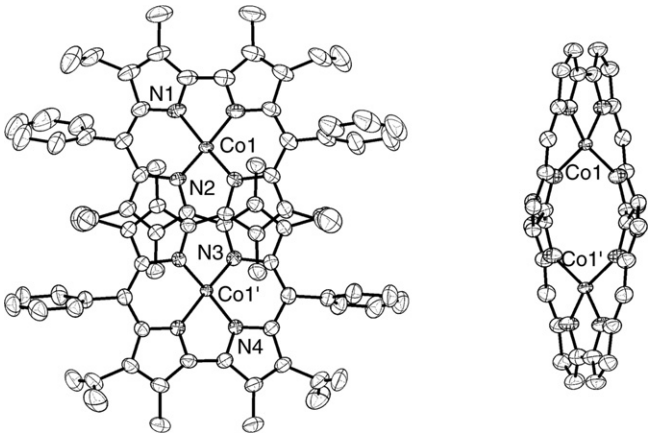


Fig. 7. 30% level Ortep drawings of **4b-Co** (left) with its side view without peripheral substituents (right). The Co atom is disordered between the two sites.

interest that Co(II) was inserted into **4a** with concomitant transposition of the 4,4′-dipropyl-2,2′-bipyrrole units from the periphery to the crossing point of the figure eight loop.

The X-ray crystallographic analysis of the monocobalt(II) complex **4b-Co** indicated the figure eight loop structure with Co(II) in a distorted tetragonal coordination geometry, although the Co atom is disordered between the two coordination sites made of four pyrrole nitrogens of the figure eight loop (see Fig. 7). The four N–Co–N angles are 84.39°, 86.49°, 86.30°, and 106.28° for the first coordi-

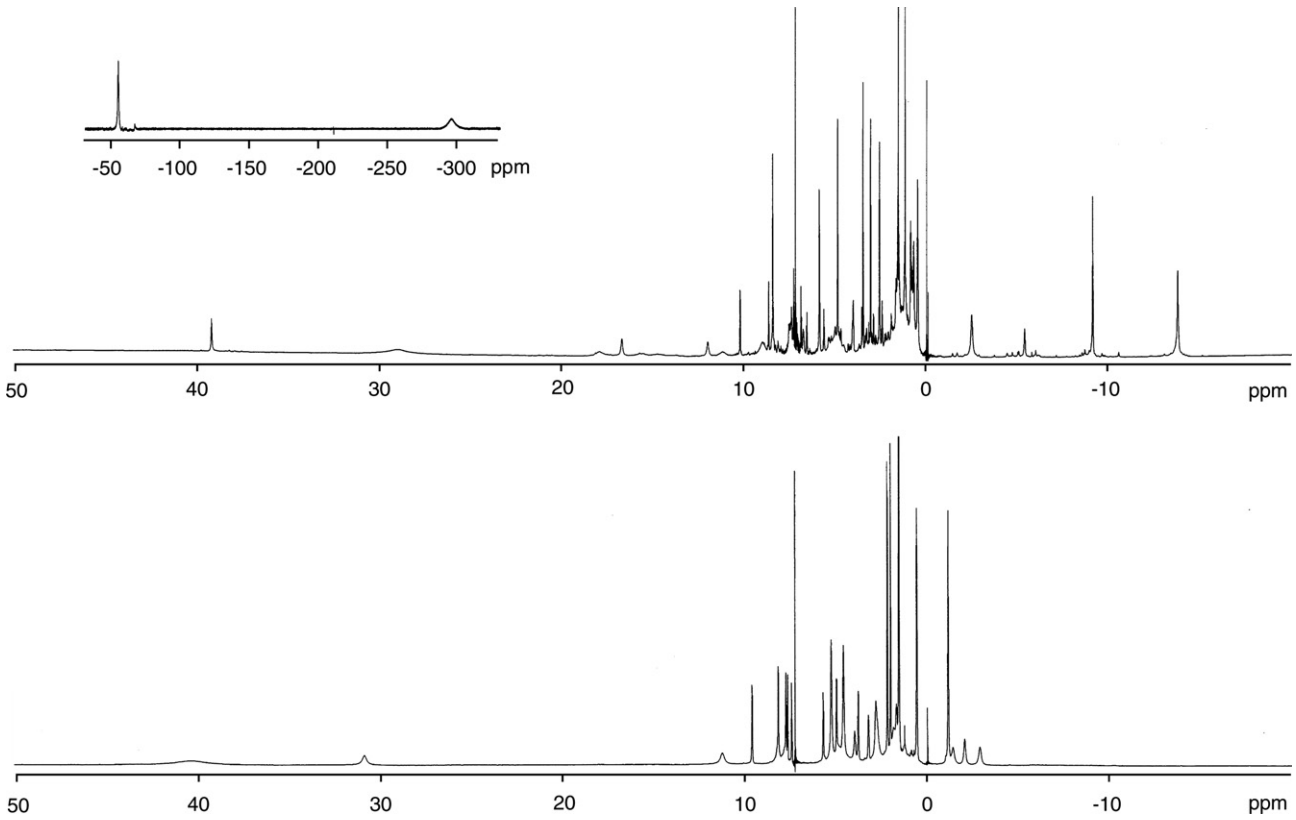


Fig. 6. $^{1}H$ NMR spectra of **4a-Co** (bottom) and **4c-Co** (top) in $CDCl_3$ at 20 °C in the chemical shift range of +50 to −20 ppm. Region of −30 to −330 ppm is shown in the inset for **4c-Co** (top).

nation site and 85.56°, 85.72°, 85.51°, and 106.86° for the second coordination site, the total sum of which are 364.04° and 363.65°, respectively. The Co–N bond lengths for the *cis*-bipyrrole units (1.848 (3), 1.856 (3), 1.842 (4), and 1.847 (4) Å) are shorter than those for the *trans*-bipyrrole units (1.966 (3), 1.977 (3), 1.996 (4), and 2.003 (4) Å). The crystal structure of **4a-Co** was also solved to give evidence in support for the positional change of the 2,2′-bipyrrole units during Co(II) insertion (see Supplementary material).

## 3. Experimental

Melting points were measured with a YANACO micro-melting point apparatus. $^1$H NMR spectra were recorded on a Varian Inova 400 spectrometer (400 MHz). Chemical shifts were referenced with respect to $(CH_3)_4Si$ (0 ppm) as an internal standard. The UV–visible spectra were measured on a JASCO V-570 spectrometer. Elemental analyses of C, H, and N were made with a YANACO MT-5 CHN recorder. ESITOF-MS spectra were measured with a Applied Biosystems Mariner mass spectrometer. Solvents were purified prior to use by conventional methods. $CDCl_3$ was passed through basic $Al_2O_3$ before use. Other chemicals were of reagent grade and used as received. 5,5′-Diformyl-4,4′-diethyl-3,3′-dimethyl-2,2′-bipyrrole and 5,5′-diformyl-4,4′-dipropyl-2,2′-bipyrrole were synthesized according to the literature method [13].

### 3.1. Syntheses

#### 3.1.1. 2,2′-Bipyrrole derivatives

*3.1.1.1. 5,5′-Bis(phenylhydroxymethyl)-2,2′-bipyrroles **2a** and **2b**.* Phenyllithium in cyclohexane–diethyl ether (5.7 ml; 5.34 mmol, 7 equiv) was added dropwise to a dry THF solution (10 ml) of 5,5′-diformyl-4,4′-dipropyl-2,2′-bipyrrole (208 mg, 0.766 mmol) cooled at −50 °C under argon. After the reaction mixture was stirred at −50 °C for 2.5 h and then at room temperature for 1 h, the resulting yellow solution was quenched with water (10 ml) showing color change to red and then to yellow. The reaction mixture was repeatedly extracted with diethyl ether. The organic layer was washed with water and then with brine. After drying over anhydrous $K_2CO_3$, the solvent was removed under reduced pressure and the residue was precipitated from cold diethyl ether–hexane to give yellow powders of 5,5′-bis(phenylhydroxymethyl)-4,4′-dipropyl-2,2′-bipyrrole **2a** as a mixture of a *meso* form and a *dl* form. **2a:** Yield 83%. $^1$H NMR ($\delta$-value in $CDCl_3$) 8.00 (br, 2H, NH); 7.36 (m, 4H, Ph–*o*-H); 7.34 (m, 4H, Ph–*m*-H); 7.28 (m, 2H, Ph–*p*-H); 5.96 (s, 2H, β-pyrrole-H); 5.95 (s, 2H, methine-H); 2.40 (t, 4H, –C*H*$_2$CH$_2$CH$_3$); 2.2 (br, 2H, OH); 1.65 (m, 4H, –CH$_2$C*H*$_2$CH$_3$); 0.98 (t, 6H, –CH$_2$CH$_2$C*H*$_3$). Anal. Calc. for $C_{28}H_{32}N_2O_2$: C, 78.47; H, 7.52; N, 6.54. Found: C, 78.59; H, 7.56; N, 6.40%. A similar procedure using 5,5′-diformyl-4,4′-diethyl-3,3′-dimethyl-2,2′-bipyrrole afforded 5,5′-bis(phenylhydroxymethyl)-4,4′-diethyl-3,3′-dimethyl-2,2′-bipyrrole **2b**: Yield 91%. $^1$H NMR ($\delta$-value in $CDCl_3$) 7.56 (br, 2H, NH); 7.38 (m, 4H, Ph–*o*-H); 7.34 (m, 4H, Ph–*m*-H); 7.28 (m, 2H, Ph–*p*-H); 5.96 (s, 2H, methine-H); 2.50 (m, 4H, –C*H*$_2$CH$_3$); 2.05 (br, 2H, OH); 1.95 (s, 6H, β-pyrrole-CH$_3$); 1.09 (m, 6H, –CH$_2$C*H*$_3$). Anal. Calc. for $C_{28}H_{32}N_2O_2$: C, 78.47; H, 7.52; N, 6.54. Found: C, 78.17; H, 7.78; N, 6.31%.

*3.1.1.2. Bis(azafulvene)s **3a** and **3b**.* To a mixture of the bipyrrole dicarbinol **2a** (270 mg, 0.633 mmol), di-*t*-butyl dicarbonate (359 mg, 1.65 mmol, 2.6 equiv), and 4-dimethylaminopyridine (3.9 mg, 0.032 mmol) was added a dry THF (10 ml) under argon. After stirring for 2 h at room temperature, the solution turned yellow. Methanol (30 ml) was added and the mixture was condensed to give precipitates of 6,6′-diphenyl-4,4′-dipropyl-2,2′-bis(azafulvene) **3a**: Yield 82%. Mp 192 °C. UV–Vis ($\lambda_{max}$ nm (log $\varepsilon$) in $CH_2Cl_2$) 416 (4.81). $^1$H NMR ($\delta$-value in $CDCl_3$) 8.37 (d, 4H, Ph–*o*-H); 7.47 (m, 4H, Ph–*m*-H); 7.43 (m, 2H, Ph–*p*-H); 7.19 (s, 2H, β-pyrrole-H); 7.08 (s, 2H, methine-H); 2.70 (t, 4H, –C*H*$_2$CH$_2$CH$_3$); 1.77 (m, 4H, –CH$_2$-C*H*$_2$CH$_3$); 1.06 (t, 6H, –CH$_2$CH$_2$C*H*$_3$). Anal. Calc. for $C_{28}H_{28}N_2$: C, 85.67; H, 7.19; N, 7.14. Found: C, 85.39; H, 7.12; N, 6.82%. A similar procedure using bipyrrole dicarbinol **2b** afforded 6,6′-diphenyl-4,4′-diethyl-3,3′-dimethyl-2,2′-bis(azafulvene) **3b**: Yield 94%. Mp 215 °C. UV–Vis ($\lambda_{max}$ nm (log $\varepsilon$) in $CH_2Cl_2$) 413 (4.76). $^1$H NMR ($\delta$-value in $CDCl_3$) 8.34 (m, 4H, Ph–*o*-H); 7.43 (m, 4H, Ph–*m*-H); 7.39 (m, 2H, Ph–*p*-H); 6.97 (s, 2H, methine-H); 2.64 (q, 4H, –C*H*$_2$CH$_3$); 2.50 (s, 4H, –CH$_3$); 1.20 (t, 6H, –CH$_2$C*H*$_3$). Anal. Calc. for $C_{28}H_{28}N_2$: C, 85.67; H, 7.19; N, 7.14. Found: C, 85.59; H, 7.18; N, 7.31%.

#### 3.1.2. Octaphyrin(1.0.1.0.1.0.1.0)s **4a** and **4b**

A dry $CH_2Cl_2$ solution (10 ml) of bis(azafulvene) **3a** (40.4 mg, 0.103 mmol) and 3,3′-di-*iso*-butyl-4,4′-dimethyl-2,2′-bipyrrole **1c** (28.6 mg, 0.100 mmol) was stirred for 20 h at room temperature. DDQ (95.3 mg, 0.42 mmol) was added to the reaction mixture and the stirring was continued for further 3 h at room temperature. The reaction mixture was passed through Celite and the filtrate was shaken with 10% aqueous NaOH solution for 3 min. The organic layer was separated, washed with water, and then dried over $Na_2SO_4$. The column chromatography on alumina with $CH_2Cl_2$ afforded octaphyrin **4a** as a purple band. Yield 28%. UV–Vis ($\lambda_{max}$ nm (log $\varepsilon$) in $CH_2Cl_2$) 377 (4.69); 553 (5.09). $^1$H NMR ($\delta$-value in toluene-$d_8$) 14.99 (br, 4H, NH); 7.75, 6.70 (d, 4H × 2, *meso*-Ph–*o*-H); 7.19, 6.91 (t, 4H × 2, *meso*-Ph–*m*-H); 7.12 (t, 4H, *meso*-Ph–*p*-H); 6.20 (s, 4H, β-pyrrole-H); 3.05, 2.95 (m, 4H × 2, –C*H*$_2$CH(CH$_3$)$_2$); 3.10 (br, 4H, –CH$_2$C*H*(CH$_3$)$_2$); 1.38, 1.01 (d × 2, 12H × 2, $J$ = 6.1, 5.8 Hz, –CH$_2$CH(C*H*$_3$)$_2$); 1.52 (s, 12H, β-pyrrole-CH$_3$); 1.65, 1.48 (m, 4H × 2, –C*H*$_2$-CH$_2$CH$_3$); 1.24, 1.23 (m, 4H × 2, –CH$_2$C*H*$_2$CH$_3$); 0.59 (t, 12H, $J$ = 6.0 Hz, –CH$_2$CH$_2$C*H*$_3$) ESI-MS (found/calcd for $C_{92}H_{104}N_8$+H$^+$) 1321.74/1321.85. Anal. Calc. for

$C_{92}H_{104}N_8 \cdot C_6H_{14}$: C, 83.59; H, 8.45; N, 7.96. Found: C, 83.72; H, 8.56; N, 7.90%. A reaction of **3b** and 4,4′-diethyl-3,3′-dimethyl-2,2′-bipyrrole **1b** was worked up similarly. Column chromatography on silica gel afforded octaphyrin **4b** by elution with $CH_2Cl_2$–acetone (20/1). Yield 39%. UV–Vis ($\lambda_{max}$ nm ($\log\varepsilon$) in $CH_2Cl_2$) 376 (4.49); 578 (4.96). $^1$H NMR ($\delta$-value in toluene-$d_8$) 15.75 (br, 4H, NH); 7.76, 7.19 (d, 4H × 2, *meso*-Ph–*o*-H); 7.47 (m, 8H, *meso*-Ph–*m*-H); 7.35 (t, 4H, *meso*-Ph–*p*-H); 2.55, 2.05 (br × 2, 12H × 2, β-pyrrole-$CH_3$); 1.97, 1.71, 1.62, 1.34 (m, 4H × 4, –C$H_2$CH$_3$); 0.73, 0.61 (t, 12H × 2, –CH$_2$C$H_3$). ESI-MS (found/calcd for $C_{84}H_{88}N_8$+$H^+$) 1210.69/1210.70. Anal. Calc. for $C_{84}H_{88}N_8$: C, 83.40; H, 7.33; N, 9.26. Found: C, 83.52; H, 7.57; N, 8.99%.

### 3.1.3. Octaphyrin(1.0.1.0.1.0.1.0) 4c

Prepared by the Rothmund type reaction of **1c** and benzaldehyde in the presence of TFA according to the synthesis of **4d** [3b]. Yield 39%. UV–Vis ($\lambda_{max}$ nm ($\log\varepsilon$) in $CH_2Cl_2$) 378 (4.31); 580 (4.81). $^1$H NMR ($\delta$-value in $CDCl_3$) 15.55 (br, 4H, NH); 7.59, 7.15 (d, 4H × 2, *meso*-Ph–*o*-H); 7.51, 7.46, 7.40 (t × 3, 4H × 3, *meso*-Ph–*m*,*p*-H); 3.6, 1.8 (br × 2, 4H × 2, –CH$_2$C$H$(CH$_3$)$_2$); 2.1 (br, 8H, –C$H_2$CH(CH$_3$)$_2$); 1.63, 1.46 (br × 2, 4H × 2, –C$H_2$CH-(CH$_3$)$_2$); 1.35, 1.23 (br × 2, 12H × 2, pyrrole-β-Me); 0.93, 0.77 (br × 2, 12H × 2, –CH$_2$CH(C$H_3$)$_2$); 0.55 (br, 24H, –CH$_2$CH(C$H_3$)$_2$). ESI-MS (found/calcd for $C_{100}H_{120}$-$N_8$+$H^+$) 1434.01/1433.97. Anal. Calc. for $C_{100}H_{120}N_8$: C, 83.75; H, 8.43; N, 7.81. Found: C, 83.38; H, 8.40; N, 7.65%.

### 3.1.4. Co(II) complexes of octaphyrin(1.0.1.0.1.0.1.0)s

#### 3.1.4.1. Mononuclear Co(II) complexes 4a-Co, 4b-Co, 4c-Co, and 4d-Co.

**4b-Co**: A mixture of octaphyrin **4b** (20 mg, 0.017 mmol), $Co(OAc)_2 \cdot 4H_2O$ (33 mg, 0.13 mmol), triethylamine (0.020 μl, 0.27 mmol), $CHCl_3$ (1.5 ml), and MeOH (0.5 ml) was stirred for 3 h at room temperature under argon. The reaction mixture was partitioned between $CH_2Cl_2$ and water. The organic layer was dried over $Na_2SO_4$ and then evaporated to dryness. The residue was chromatographed on alumina with hexane–$CH_2Cl_2$ (3/1) to give a blue fraction. Recrystallization from hexane–$CH_2Cl_2$ afforded the monocobalt complex **4b-Co**. Yield 66%. UV–Vis ($\lambda_{max}$ nm ($\log\varepsilon$) in $CH_2Cl_2$) 588 (4.91). $^1$H NMR ($\delta$-value in $CDCl_3$) summarized in Table 2. ESI-MS (found/calcd for $C_{84}H_{86}N_8Co$+$H^+$) 1266.69/1266.64. Anal. Calc. for $C_{84}H_{86}N_8Co \cdot CH_2Cl_2 \cdot C_6H_{14}$: C,76.02; H, 7.15; N, 7.79. Found: C, 75.54; H, 7.06; N, 7.63%.

**4a-Co**: Yield 57%. UV–Vis ($\lambda_{max}$ nm ($\log\varepsilon$) in $CH_2Cl_2$) 581 (4.85). $^1$H NMR ($\delta$-value in $CDCl_3$) 40.5 (NH); 30.8, 11.3 (–C$H_2$CH(CH$_3$)$_2$); 9.6, 8.2, 7.8, 7.7, 7.5 (*meso*-Ph–H); 5.8, 5.0, 4.0, 3.8, 3.2, 2.8, 1.7, −1.4, −2.0, −2.8 (*meso*-Ph–H and alkyl-H); 5.3, 4.6 2.8, 2.2, 2.0, 1.6, 0.6, −1.2 ($CH_3$). ESI-MS (found/calcd for $C_{92}H_{102}N_8$+$H^+$) 1378.67/1378.76. Anal. Calc. for $C_{92}H_{102}N_8Co \cdot 2H_2O$: C, 78.10; H, 7.55; N, 7.92. Found: C, 77.63; H, 7.38; N, 7.93%.

**4c-Co**: Yield 59%. UV–Vis ($\lambda_{max}$ nm ($\log\varepsilon$) in $CH_2Cl_2$) 584 (4.90). $^1$H NMR ($\delta$-value in $CDCl_3$) 39.2 (NH); 29.0, 11.0 (–C$H_2$CH(CH$_3$)$_2$); 10.2, 8.6, 7.3, 6.9, 6.6 (*meso*-Ph–H); 17.9, 16.6, 9.0, 7.4, 6.8, 4.1, 4.0, 2.6, 1.7, −2.5, −5.4 (*meso*-Ph–H and alkyl-H); 8.4, 5.9, 4.9, 3.5, 3.1, 2.6, 0.9, 0.7, 0.5, −9.1, −13.9 ($CH_3$); −54.5, −293.8 (–C$H_2$CH-(CH$_3$)$_2$). ESI-MS (found/calcd for $C_{100}H_{118}N_8Co$+$H^+$) 1490.73/1490.89. Anal. Calc. for $C_{100}H_{118}N_8Co$: C, 83.46; H, 7.49; N, 9.05. Found: C, 83.29; H, 7.36; N, 9.33%.

**4d-Co**: Yield 45%. UV–Vis ($\lambda_{max}$ nm ($\log\varepsilon$) in $CH_2Cl_2$) 580 (4.94). $^1$H NMR ($\delta$-value in $CDCl_3$) 42.1 (NH); 27.8, 18.6, 16.8, 16.4, 11.5, 10.7, 6.5, 5.8, 5.3, 4.2, 2.2, −1.5, −2.4, −3.1, −6.4, −7.4, −35.5, −205 (–C$H_2$CH$_3$ and *meso*-Ph–H); 13.8, 7.9, 4.1, 3.0, 0.5, −1.5, −4.8, −19.3 (–CH$_2$C$H_3$); 10.1, 9.3 (Ph–*o*-H); 7.4, 7.2, 7.1, 4.7, 3.5, 2.7 (*meso*-Ph–*m*,*p*-H). ESI-MS (found/calcd for $C_{92}H_{102}N_8$-Co+$H^+$) 1378.61/1378.76. Anal. Calc. for $C_{92}H_{102}N_8$-$Co \cdot 2CHCl_3$: C, 69.80; H, 6.48; N, 6.93. Found: C, 70.65; H, 6.67; N, 7.09%.

#### 3.1.4.2. Dinuclear Co(II) complexes 4b-Co$_2$ and 4d-Co$_2$.

A mixture of octaphyrin **4b** (20 mg, 0.017 mmol), $Co(acac)_2$ (39 mg, 0.13 mmol), and phenol (1.0 g) was heated at reflux for 3 h under argon. The reaction mixture was partitioned between $CH_2Cl_2$ and 0.5 N aqueous NaOH solution. The organic layer was dried over $Na_2SO_4$ and then evaporated to dryness. The residue was chromatographed on alumina with $CH_2Cl_2$–acetone (2/1) to give a blue fraction. Recrystallization from hexane–$CH_2Cl_2$ afforded the dicobalt complex **4b-Co$_2$**. Yield 28%. UV–Vis ($\lambda_{max}$ nm ($\log\varepsilon$) in $CH_2Cl_2$) 392 (4.68); 597 (4.87). $^1$H NMR ($\delta$-value in $CDCl_3$) summarized in Table 2. ESI-MS (found/calcd for $C_{84}H_{84}N_8Co_2$) 1322.35/1322.55. Anal. Calc. for $C_{84}H_{84}N_8Co_2 \cdot CH_2Cl_2 \cdot C_6H_{14}$: C,73.13; H, 6.74; N, 7.50. Found: C, 72.84; H, 6.46; N, 7.41%.

**4d-Co$_2$**: Yield 33%. UV–Vis ($\lambda_{max}$ nm ($\log\varepsilon$) in $CH_2Cl_2$) 592 (4.74). $^1$H NMR ($\delta$-value in $CDCl_3$) summarized in Table 2. ESI-MS (found/calcd for $C_{92}H_{100}N_8Co_2$) 1435.55/1435.67. Anal. Calc. for $C_{92}H_{100}N_8Co_2 \cdot 2CHCl_3$: C, 67.43; H, 6.14; N, 6.69. Found: C, 67.08; H, 6.07; N, 6.71%.

## 3.2. X-ray crystallography

Bruker Smart 1000 diffractometer equipped with a CCD detector was used for data collection. An empirical absorption correction was applied using the SADABS program. The structure was solved and refined by full-matrix least-squares calculations on $F^2$ using the SHELXTL 97 program package [14]. The hydrogen atoms were included at standard positions but not refined.

Recrystallization from $CH_2Cl_2$/hexane gave crystals of **4a**. Crystal data: $C_{92}H_{104}N_8 \cdot C_6H_{14}$, $M = 1408.00$, monoclinic, space group $P2(1)/n$, $a = 16.856(2)$, $b = 28.935(4)$, $c = 17.283(2)$ Å, $\beta = 92.182(2)°$, $V = 8423.6(18)$ Å$^3$, $Z = 4$, $D_{calc} = 1.110$ Mg/m$^3$, $\mu$(Mo-K$\alpha$) = 0.064 mm$^{-1}$, $T = 293(2)$ K, crystal size 0.60 × 0.40 × 0.30 mm. A total of 17,402 unique reflections were collected ($2.8 < 2\theta < 54.7°$) using graphite-monochromated Mo-K$\alpha$ radiation. 985 para-

meters were refined with all non-hydrogen atoms anisotropically. All hydrogen atoms placed at ideal positions were included but not refined. $R_1 = 0.975$, $wR_2 = 0.2459$ for 7281 reflections with $I > 2.00\sigma(I)$; $R_1 = 0.2125$, $wR_2 = 0.3183$ for all data. GOF (on $F^2$) = 1.005.

Recrystallization from $CH_2Cl_2$/pentane gave crystals of **4b-Co**. Crystal data: $C_{84}H_{86}N_8Co \cdot 2C_5H_{12}$, $M = 1410.83$, triclinic, space group $P\bar{1}$, $a = 13.9511(10)$, $b = 13.9536(10)$, $c = 20.7904(15)$ Å, $\alpha = 82.0170(10)°$, $\beta = 82.0600(10)°$, $\gamma = 86.0630(10)°$, $V = 3965.3(5)$ Å$^3$, $Z = 2$, $D_{calc} = 1.182$ Mg/m$^3$, $\mu$(Mo-K$\alpha$) = 0.268 mm$^{-1}$, $T = 293(2)$ K, crystal size $0.4 \times 0.3 \times 0.2$ mm. A total of 15,040 unique reflections were collected ($2.0 < 2\theta < 54.4°$) using graphite-monochromated Mo-K$\alpha$ radiation. 930 parameters were refined with all non-hydrogen atoms for the octaphyrin moiety anisotropically. C(85) to C(94) belonging to pentane solvates were refined isotropically. All hydrogen atoms placed at ideal positions were included but not refined. Refined occupancies for the disordered Co(1)/Co(2), C(39A)/C(39B), and C(59A)/C(59B) were 0.54/0.46, 0.56/0.44, and 0.58/0.42, respectively. $R_1 = 0.0832$, $wR_2 = 0.2284$ for 9272 reflections with $I > 2.00\sigma(I)$; $R_1 = 0.1355$, $wR_2 = 0.2729$ for all data. GOF (on $F^2$) = 1.069.

## 4. Summary

The free bases and Co(II) complexes of *meso*-tetraphenyloctaphyrin(1.0.1.0.1.0.1.0)s were unambiguously characterized on the basis of the $^1$H NMR spectra and X-ray crystallography. The octaphyrin having alternate arrangement of two 2,2′-bipyrroles with different stereochemical feature was synthesized without scrambling. Although the *iso*-butyl-substituted 2,2′-bipyrrole was at the crossing point of the figure eight loop in the free base octaphyrin, transposition of the 2,2′-bipyrrole unit led to the exclusive formation of the Co(II) complex where the propyl-substituted bipyrrole is at the crossing point. The structural feature of this Co(II) octaphyrin is preferable for studying coordination chemistry because Co(II) is not covered by alkyl groups at the pyrrole β-position.

## Acknowledgements

This work was supported by Grant-in-Aid for Scientific Research (Nos. 16350023 and 16033240) from the Ministry of Education, Culture, Sports, Science and Technology, Japan. The author is also grateful to the CREST program (the Japan Science and Technology Agent) and the VBL project (Kobe University). The authors are also grateful to Prof. K. Eda (Kobe Univ.) for his help in the X-ray crystallographic analysis.

## Appendix A. Supplementary data

Crystallographic data for the structural analyses have been deposited with the Cambridge Crystallographic Data Center, CCDC reference numbers for **4a**, **4b-Co**, and **4a-Co** are 603485, 603486 and 603487, respectively. Copies of this information may be obtained free of charge from The director, CCDC, 12 Union Road, Cambridge, CB2 1EZ UK (fax: +44 1223 336033; e-mail: deposit@ccdc.cam.ac.uk or www: http://www.ccdc.cam.ac.uk). Detailed crystallographic data of **4a**, **4b-Co**, and **4a-Co** with their Ortep drawings and a 2D ROESY NMR spectrum of **4a** were included. Supplementary data associated with this article can be found, in the online version, at doi:10.1016/j.jorganchem.2006.04.045.

## References

[1] (a) J.L. Sessler, D. Seidel, Angew. Chem., Int. Ed. 42 (2003) 5134;
(b) L. Latos-Grażyński, Angew. Chem., Int. Ed. 43 (2004) 5124;
(c) T.D. Lash, Angew. Chem. Int. Ed. 39 (2000) 1763;
(d) J.L. Sessler, A. Gebauer, S.J. Weghorn, in: K.M. Kadish, K.M. Smith, R. Guilard (Eds.), The Porphyrin Handbook, vol. 2, Academic Press, New York, 2000, p. 55.

[2] (a) J.L. Sessler, S.J. Weghorn, T. Morishima, M. Rosingana, V. Lynch, V. Lee, J. Am. Chem. Soc. 114 (1992) 8306;
(b) J.L. Sessler, S.J. Weghorn, V. Lynch, M.R. Johnson, Angew. Chem., Int. Ed. 33 (1994) 1509;
(c) M. Bröring, J. Jendrny, L. Zander, H. Schmickler, J. Lex, Y.D. Wu, M. Nendel, J.G. Chen, D.A. Plattner, K.N. Houk, E. Vogel, Angew. Chem., Int. Ed. 34 (1995) 2515;
(d) J.-Y. Shin, H. Furuta, K. Yoza, S. Igarashi, A. Osuka, J. Am. Chem. Soc. 123 (2001) 7190.

[3] (a) J. Setsune, S. Maeda, J. Am. Chem. Soc. 122 (2000) 12405;
(b) J. Setsune, Y. Katakami, N. Iizuna, J. Am. Chem. Soc. 121 (1999) 8957;
(c) J. Setsune, A. Tanabe, J. Watanabe, S. Maeda, Org. Biomol. Chem. 4 (2006) 2247.

[4] A. Werner, M. Michels, L. Zander, J. Lex, E. Vogel, Angew. Chem., Int. Ed. 38 (1999) 3650.

[5] E. Vogel, M. Michels, L. Zander, J. Lex, N.S. Tuzum, K.N. Houk, Angew. Chem., Int. Ed. 42 (2003) 2857.

[6] T. Köhler, M.C. Hodgson, D. Seidel, J.M. Veauthier, S. Meyer, V. Lynch, P.D.W. Boyd, P.J. Brothers, J.L. Sessler, Chem. Commun. 9 (2004) 1060.

[7] Y. Tanaka, W. Hoshino, S. Shimizu, K. Youfu, N. Aratani, N. Maruyama, S. Fujita, A. Osuka, J. Am. Chem. Soc. 126 (2004) 3046.

[8] S. Shimizu, Y. Tanaka, K. Youfu, A. Osuka, Angew. Chem., Int. Ed. 44 (2005) 3726.

[9] (a) J. Bley-Escrich, J.-P. Gisselbrecht, M. Michels, L. Zander, E. Vogel, M. Gross, Eur. J. Inorg. Chem. (2004) 492;
(b) J.P. Gisselbrecht, J. Bley-Escrich, M. Gross, L. Zander, M. Michels, E. Vogel, J. Electroanal. Chem. 469 (1999) 170;
(c) J. Bley-Escrich, J.P. Gisselbrecht, E. Vogel, M. Gross, Eur. J. Inorg. Chem. (2002) 2829.

[10] (a) B.J. Litter, Y. Ciringh, J.S. Lindsey, J. Org. Chem. 64 (1999) 2864;
(b) J.S. Lindsey, in: K.M. Kadish, K.M. Smith, R. Guilard (Eds.), The Porphyrin Handbook, vol. 1, Academic Press, New York, 2000, pp. 45–118.

[11] J. Setsune, A. Tsukajima, J. Watanabe, Tetrahedron Lett. 47 (2006) 1817.

[12] G.N. La Mar, F. Ann Walker, J. Am. Chem. Soc. 95 (1973) 1790.

[13] (a) J.L. Sessler, M.J. Cyr, V.L. Lynch, J. Am. Chem. Soc. 121 (1990) 2810;
(b) E. Vogel, M. Belci, K. Pramod, P. Koch, J. Lex, O. Ermer, Angew. Chem., Int. Ed. Engl. 26 (1987) 928.

[14] G.M. Sheldrick, SHELXTL 5.10 for Windows NT: Structure Determination Software Programs, Bruker Analytical X-ray Systems, Inc., Madison, WI, 1997.